Title

Authigenic carbonate formation rates in marine sediments and implications for the marine δ 13C record

Authors

Mitnick, Elizabeth H
Lammers, Laura N
Zhang, Shuo
et al.

Publication Date

2018-08-01

DOI

10.1016/j.epsl.2018.05.018

Peer reviewed

Authigenic carbonate formation rates in marine sediments and implications for the marine $\delta^{13}C$ record

Elizabeth H. Mitnick[a] Laura N. Lammers[cb] Shuo Zhang[d] Yan Zaretskiy[d] Donald J. DePaolo[ab]

Abstract

Carbon isotope (δ13C) variations measured in carbonates have been attributed to large-scale phenomena throughout Earth history, such as changes in atmospheric oxygen or global glaciations. These interpretations follow from a model wherein the δ13C of marine dissolved inorganic carbon (DIC) is controlled by the relative sedimentary burial rates of biogenic carbonate (BC) and organic carbon (OC). A new model proposes authigenic carbonate (AC) as a third major sedimentary C pool, implying that δ13C anomalies are not necessarily indicative of extreme changes in the global carbon cycle and/or atmospheric oxygen. Two conditions are required for AC formation to significantly alter bulk carbonate δ13C: the AC isotopic composition must be at least ~3‰ different from that of BC and the AC/BC ratio must be >0.1. We use pore fluid Ca and Sr concentrations to estimate rates of AC formation in Late Cenozoic marine sediments, then calculate relative fractions of AC, OC, and BC. Today AC is not expected to constitute a significant fraction of total sedimentary carbon (AC+OC+BC) globally; however, there are modern sites where local conditions promote elevated AC/BC and anaerobic metabolisms can alter the δ13C of pore fluids. We investigate these sites to determine what conditions might enable AC to alter δ13C of marine DIC. We find there is very little net addition of AC relative to BC, but large quantities of AC form today across many settings via recrystallization. In settings where remineralization of organic matter causes recrystallized carbonate to form with modified δ13C, AC/BC is generally too low for this recrystallization to significantly shift the δ13C of the bulk carbonate. However, exceptions are found in sites with very low BC and extensive methane oxidation, suggesting that this environment type would need to be globally extensive in the past in order for AC formation to change the δ13C of marine DIC.

Keywords: authigenic carbonate, marine sediments, carbon isotopes, carbon cycle

1. Introduction

1.1. Overview

A longstanding problem in the study of paleoclimate lies in explaining carbon isotope (C) variation in the geologic record, thought to reflect changes in the C of marine dissolved inorganic carbon (M-DIC) through Earth history (Fig. 1). In this record, there are both long-term (>10^7 yr) and transient variations (±3‰ or larger) that persist for periods extending beyond the 0.1 My residence time of M-DIC (e.g., Halverson et al., 2005, Kump and Arthur,

1999, Payne et al., 2004, Saltzman, 2005, Saltzman and Thomas, 2012, Sephton et al., 2002, Shields and Veizer, 2002). The traditional interpretation of the $C_{M\text{-}DIC}$ record is based on a steady-state mass balance between carbon inputs (C_{in}) to the M-DIC reservoir and the relative sedimentary burial rates of carbonate carbon and organic carbon(e.g., Arthur et al., 1988, Canfield and Kump, 2013), written as:

(1)

where *f* represents the fraction of total sedimentary carbon that is either carbonate (*carb*) or organic carbon (*org*). Organic carbon has a much lower C relative to that of M-DIC due to fractionation during photosynthesis and other carbon fixation pathways. The $C_{M\text{-}DIC}$ is assumed to be roughly equal to C_{carb}, as there is only a small fractionation between M-DIC and carbonate. There are spatial variations in $C_{M\text{-}DIC}$ (up to ~3‰) due to temperature-dependent circulation effects as well as biological productivity, fluxes of organic matter to the deep ocean, and remineralization rates (e.g., Raven and Falkowski, 1999), although deep water values average 0‰, with modern mean $C_{M\text{-}DIC}$ equal to (Saltzman and Thomas, 2012).

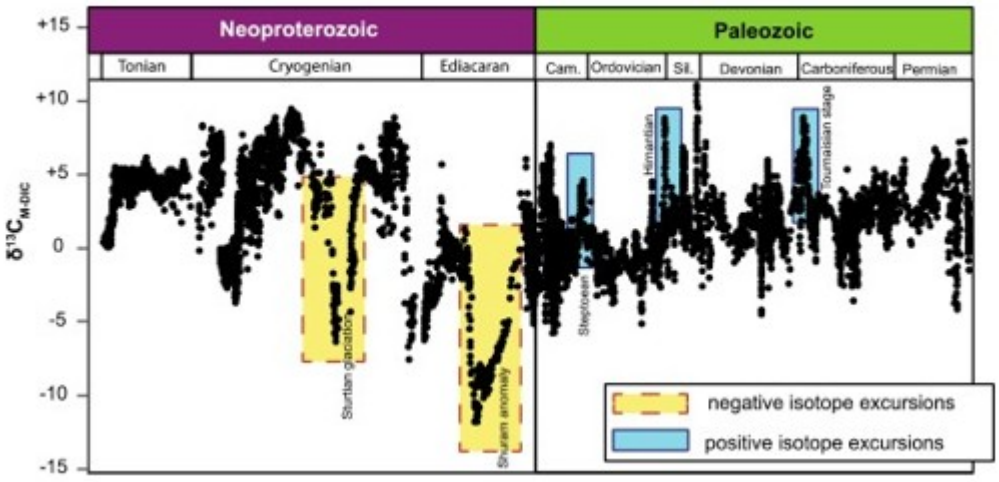

Fig. 1. Neoproterozoic and Paleozoic marine carbon isotope record. Some examples of isotope excursions highlighted in yellow with dashed line (negative excursions) and blue with solid line (positive excursions). Data from Halverson et al. (2005) and Saltzman and Thomas (2012).

1.2. Use of the record as a paleoproxy for oxygenation state

The C record has been used in the context of equation (1) as a proxy for atmospheric oxygen production and removal due to burial or consumption of organic carbon. This proxy is based on the relationship between organic carbon and oxygen during aerobic respiration (Eq. (2); Berner and Canfield, 1989, Berner and Maasch, 1996) according to the reaction,

(2)

Following this relationship, if , the organic carbon burial fraction, increases for an extended period of time, atmospheric oxygen is expected to build up.

Similarly, atmospheric oxygen levels should decrease if the organic carbon burial rate decreases for an extended period of time (e.g., Berner and Petsch, 1998).

There exists a substantial body of work that attempts to constrain atmospheric oxygen levels in the past, based on evidence including distribution of redox-sensitive elements such as molybdenum, uranium, and iron, as well as sulfur isotopes and phylogenetic clues (Berner and Canfield, 1989, Canfield and Teske, 1996; Farquar et al., 2001; Lowenstein et al., 2014and references therein). However, there are places in the record, some of which are summarized by Schrag et al. (2013), where the O_2-interpretation of the C signal is at odds with other proxies and observations, lacks independent evidence, or implies much larger changes than are likely. Consequently, other explanations for patterns in C have been proposed.

An altered oxygenation state of the Earth's atmosphere and oceans is not the only interpretation of the $C_{M\text{-}DIC}$ record, although many proposed interpretations are at least indirectly tied to an altered global redox environment. There are large magnitude excursions associated with glaciations (e.g., Marshall et al., 1997), mass extinctions (e.g., Sephton et al., 2002), ocean anoxic events (e.g., Arthur et al., 1988), consequences of emplacement of large igneous provinces (e.g., Retallack and Jahren, 2008), as well as inferred events such as the catastrophic release of methane clathrates (e.g., Dickens et al., 1995). However, there are isotope excursions in the record, such as those identified by Schrag et al. (2013), that do not have other geochemical or stratigraphic indicators of global change, specifically changes in oxygenation state, and these excursions therefore cannot be interpreted with any degree of confidence.

1.3. Considering authigenic carbonate in the carbon isotope mass balance

Motivated by inconsistencies between the C record and evidence from other proxy records, alternative models have been proposed that would serve to decouple atmospheric O_2 from seawater C. One of these models posits that carbonate formed within marine sediments, called authigenic carbonate (AC), could take on values of C and form at high enough rates relative to the organic C and biogenic carbonate burial fluxes, such that $C_{M\text{-}DIC}$ could shift without requiring a large change in atmospheric oxygen (Schrag et al., 2013). This mechanism could then cause variations in $C_{M\text{-}DIC}$ that are no longer directly tied to the CO_2–O_2 balance. In the marine environment, AC forms within sediments, either by (a) “recrystallization”, which is dissolution of biogenic carbonates (“BC”; i.e., detrital tests of forminifers or coccoliths) followed by reprecipitation as nonbiogenic carbonate, or (b) net precipitation from pore fluids due to an increase in carbonate alkalinity caused by microbial respiration of organic carbon or methane (Morse et al., 2007), or alternatively due to deepening of the carbonate compensation depth (CCD) to well below the sediment–water interface.

The steady-state C mass balance described by Eq. (1) has been rewritten by Schrag et al. (2013) to include AC in addition to the original sedimentary C sinks, biogenic carbonate (BC) and organic carbon (OC):

(3)

(4)

where ε indicates the fractionation factor between M-DIC and the sedimentary carbon pool (e.g., if , C_{OC} =). According to these formulae, two conditions must be met for AC to be important to the overall isotopic mass balance and to cause changes to $C_{M\text{-}DIC}$. First, f_{AC} must be similar in magnitude to f_{BC} and f_{OC}. Second, must be different from , or Eq. (3) reduces to Eq. (1). As written in Eq. (4), the value of $C_{M\text{-}DIC}$ depends on the sedimentary fractions and fractionation factors for AC, OC, and BC, as well as the isotopic inputs to the M-DIC pool.

For the AC term to be significant in equation (4), not only must f_{AC} be sufficiently large, but the AC isotopic composition must also be significantly different from that of BC. Herein we define AC that is isotopically different from ‰ as AC*, and $*$ is the corresponding sedimentary carbon fraction. Where the isotopic composition of AC does not deviate from that of BC, or in cases where authigenic carbonate is discussed independently of its isotopic composition, ‘AC’ is used.

The long-term average value of is estimated as ~0.2 (Schidlowski et al., 1975, Derry, 2014), and this value is associated with a relatively stable amount of atmospheric O_2 during the Phanerozoic. If we want to determine how great an effect AC could have while maintaining our modern atmospheric oxygen level, we set the constraint of = 0.2, which results in:

(5)

Steady state conditions of = 0 and = 0.2 result in our modern $C_{M\text{-}DIC}$ value of ~0 (following Eq. (4)). If we assume that scales with production/removal of O_2, then to evaluate what is required to have $C_{M\text{-}DIC}$ vary without changing pO_2, we hold constant in equation (4). To generate $|C_{M\text{-}DIC}| > 3$ due to AC formation without changing the burial fraction of OC (and consequently, atmospheric O_2), the fractions of BC and AC must sum to 0.8, with less AC required when is large, and more AC required when is small (Fig. 2).

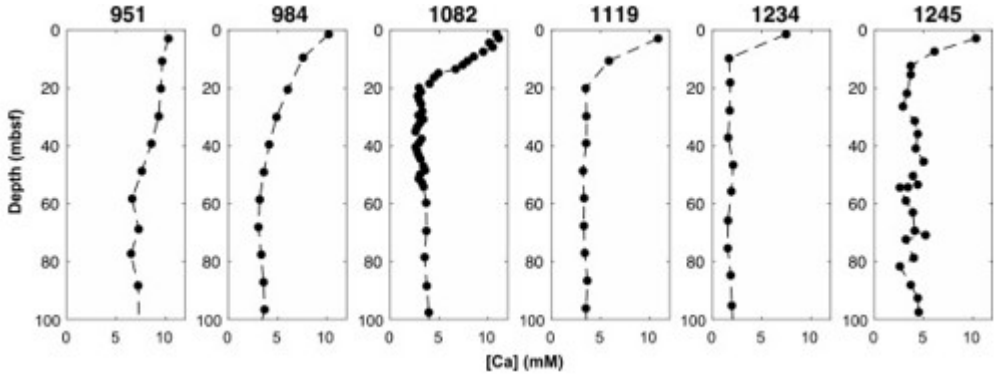

Fig. 2. Pore fluid calcium concentrations (mM) for examples of Type I sites (<65 wt% carbonate and OC/(AC + BC) > 0.1.

1.4. Aims and approach of present study

There has been increasing interest over the past years to understand the role and nature of authigenic carbonate in both modern and ancient sediments (Canfield and Kump, 2013, Schrag et al., 2013, Sun and Turchyn, 2014). However, sedimentary carbon fluxes from AC precipitation have not been evaluated in the context of coeval biogenic carbonate and organic carbon fluxes, nor have the AC fluxes been considered in an isotopic context. This contextual assessment of authigenic carbonate is crucial if we are to understand how the burial dynamics of marine carbonate play into the carbon cycle and affect the steady-state isotopic composition of the ocean. Schrag et al. (2013) and numerous other studies also raise the question of whether or not the C record is recording global versus local marine signals, and we explore this in our discussion as well.

In this study, we quantify modern-day carbon isotope fluxes due to AC formation in a variety of different marine sedimentary environments. Although globally, it is not expected that AC is a significant fraction of total sedimentary carbon today, there are a wide variety of sedimentary environments represented by cores collected through the International Ocean Discovery Program (IODP), including sites known or thought to have considerable AC production locally. Sites with significant $*$ might provide insight into global sedimentary conditions that could have shifted $C_{M\text{-}DIC}$ in the past. We then estimate the range of isotopic values of AC based on known mechanisms supported by pore fluid profiles of $\delta 13C_{PF\text{-}DIC}$ and δ13C of bulk carbonates. We discuss possible controls on authigenic carbonate formation in marine sediments and implications of our results for understanding the role of authigenic carbonate in the δ13C record, and interpreting δ13C as a record of global phenomena.

2. Methods

2.1. Overview

Reactions within marine sediments are reflected in pore fluid concentrations of Ca2+,Mg2+,Sr2+,HCO3−,SO42− as well as pH and other variables. Our

objective is to use pore fluid chemistry to estimate rates of authigenic carbonate formation. This is accomplished using depth-variant pore fluid Ca and Sr concentrations within a one-dimensional diffusion–advection–reaction model. The marine sediment cores in our study were selected from the International Ocean Discovery Program as well as sites from preceding ocean drilling initiatives (Deep Sea Drilling Project (1966–1983), Ocean Drilling Program (1983–2003), and Integrated Ocean Drilling Program (2003–2013), summarized in Table 1. Site data is sourced from the online repository (link in Supplemental Material) as well as from individual site reports (see Supplemental Material for references by site). This approach is useful to determine how AC formation rate varies with sedimentation conditions, and will allow us to learn about what conditions could represent times in Earth history with globally high AC production. The limitation on the number of sites (N=37) is due to data availability and the fineness of the spatial resolution of measurements.

Table 1. Summary of sites included in this study.

DSDP/ODP/ IODP Leg	Site	Water depth (m)	Expedition	Description
42	381	1728	Black Sea	Anoxic bottom waters
96	618	2412	Orca Basin	Anoxic bottom waters
112	681	150.5	Peru Continental Margin	Continental shelf
112	688	3827	Peru Continental Margin	Continental margin
113	693	2359	Weddell Sea, Antarctica	Continental margin
117	725	311.5	Oman Margin	Oxygen minimum zone
130	803	3410	Ontong Java Plateau	Deep-sea
130	805	3189	Ontong Java Plateau	Deep-sea
130	806	2520	Ontong Java Plateau	Deep-sea
130	807	2804	Ontong Java Plateau	Deep-sea

DSDP/ODP/ IODP Leg	Site	Water depth (m)	Expedition	Description
133	819	565	Northeast Australian Margin	Continental slope
139	855	2445	Middle Valley, Juan de Fuca Ridge	Deep-sea
141	860	2148	Chile Triple Junction	Continental margin
141	863	2564	Chile Triple Junction	Continental margin
146	892	675	Cascadia Margin	Continental margin
157	950	5437	Gran Canaria and Madeira Abyssal Plain	Deep-sea
157	951	5437	Gran Canaria and Madeira Abyssal Plain	Deep-sea
162	984	1649	North Atlantic–Arctic Gateways II	Deep-sea
165	998	3180	Caribbean Ocean History	Continental margin
165	999	2828	Caribbean Ocean History	Continental

DSDP/ODP/ IODP Leg	Site	Water depth (m)	Expedition	Description
				margin
166	1003	481.4	Bahamas Transect	Carbonate platform
169S	1033	203	Saanich Inlet	Anoxic fjord
169S	1034	226	Saanich Inlet	Anoxic fjord
175	1082	1279	Benguela Current	Upwelling zone
175	1084	1992	Benguela Current	Upwelling zone
177	1088	2082	Southern Ocean Paleoceanorgraphy	Deep-sea
177	1092	1974	Southern Ocean Paleoceanorgraphy	Deep-sea
181	1119	393	Southwest Pacific Gateways	Continental slope
181	1120	543	Southwest Pacific Gateways	Continental margin
189	1169	3568	Tasmanian Gateway	Deep-sea

DSDP/ODP/ IODP Leg	Site	Water depth (m)	Expedition	Description
194	1194	368	Marion Plateau, Northeast Australia	Carbonate platform
202	1232	4072	Southeast Pacific Paleoceanographic Transects	Continental margin
202	1234	1015	Southeast Pacific Paleoceanographic Transects	Continental slope
204	1245	870	Cascadia Continental Margin	Continental margin
313	M0027	32	New Jersey Shallow Shelf	Continental shelf
347	M0059	37	Baltic Sea Basin	Shallow basin
308	U1319	1430	Brazos–Trinity Basin IV (Gulf of Mexico)	Continental slope

2.2. Modeling approach

2.2.1. Site categorization and estimation of absolute AC formation rates

The term “authigenic” means “formed in place” and hence strictly speaking, refers to any carbonate formed within the sediment after deposition. Recognizing that authigenic carbonate (*sensu lato*) encompasses the net addition of carbonate to sediments (or the sediment–water interface) via remineralization of organic matter as well as the replacement of primary sedimentary carbonate (dominantly biogenic in the modern era), we have used two different approaches to estimating precipitation rates for these end-member types of AC formation.

Many sediment cores have a net decrease in porewater calcium with depth (Fig. 2). This feature generally corresponds to sites with <65 wt% carbonate and high pore fluid alkalinity, as well as high ratios of OC to carbonate (Table 2). These ‘Type I’ sites often show complete net sulfate removal from modern seawater levels of ~28 mM (Walter et al., 1993), suggesting high rates of sulfate reduction within the upper tens of meters. High sulfate reduction rates coupled to the oxidation of a light-δ13C source, indicates that these sites will have low-δ13C pore fluids. The extent of organic matter remineralization can often be inferred from alkalinity profiles as well, because the anaerobic oxidation of organic matter generates carbonate alkalinity. The pore fluid geochemistry at these sites – specifically the net removal of Ca coupled to the depletion of sulfate – makes them excellent candidates to calculate net precipitation of AC directly from Ca concentrations.

Table 2. Sites included in this study categorized as Type I or Type II sites. Exceptions denoted with '*' and discussed in section SI.6 of Supplemental Material. Range of total alkalinity (TA) measured in pore fluids over the top ~80 m of sediment. X_{carb} = kg carbonate/kg sediment and X_{oc} = kg organic carbon/kg sediment averaged over the top ~80 m.

Leg	**Site**	**TA (*low*) (mM)**	**TA (*high*) (mM)**	**X_{carb}**	**X_{oc}**	**X_{oc}/X_{carb} (%)**	**Type**
165	998	2.96	4.73	0.72	0	0	II
130	805	2.9	5.36	0.91	0.001	0.11	II
177	1088	2.76	3.89	0.91	0.001	0.11	II
130	807	3.51	4.68	0.92	0.001	0.13	II
181	1120	2.74	4.6	0.95	0.002	0.19	II
177	1092	2.51	3.69	0.8	0.002	0.2	II
130	803	3.23	3.76	0.89	0.002	0.2	II
130	806	3.73	5.8	0.91	0.002	0.23	II
165	999	3.57	5.15	0.5	0.001	0.26	*

Leg	Site	TA (*low*) (mM)	TA (*high*) (mM)	X_{carb}	X_{oc}	X_{oc}/X_{carb} (%)	Type
189	1169	3.98	5.84	0.85	0.003	0.39	II
194	1194	1.92	2.94	0.79	0.004	0.46	II
133	819	2.80	4.4	0.52	0.004	0.73	*
166	1003	2.17	26.03	0.94	0.008	0.88	II
117	725	3.67	17.31	0.54	0.007	1.28	I
157	951	3.26	4.96	0.49	0.008	1.67	I
157	950	4.1	6.2	0.58	0.01	1.72	I
162	984	3.98	14.18	0.16	0.003	1.79	I
202	1234	10.95	72.84	0.4	0.013	3.15	I
181	1119	2.18	27.73	0.09	0.003	3.78	I
308	U1319	2.95	19.45	0.15	0.00	5.07	I

Leg	Site	TA (*low*) (mM)	TA (*high*) (mM)	X_{carb}	X_{oc}	X_{oc}/X_{carb} (%)	Type
					8		
42	381	4.64	18.1	0.17	0.01	5.88	I
113	693	3.49	3.9	0.02	0.002	7.5	I
139	855	2.03	10.36	0.06	0.005	7.67	I
204	1245	8.26	67.83	0.1	0.009	8.9	I
202	1232	23.44	36.45	0.02	0.002	9	I
175	1082	2.02	74.32	0.48	0.051	10.53	I
96	618	6.46	21.54	0.08	0.01	12.5	I
347	M0059	4.2	206.1	0.17	0.034	20.26	I
313	M0027	1.07	4.02	0.02	0.004	21.39	I
175	1084	4.07	171.67	0.36	0.084	23.31	I

Leg	Site	TA (*low*) (mM)	TA (*high*) (mM)	X_{carb}	X_{oc}	X_{oc}/X_{carb} (%)	Type
112	688	28.44	189.27	0.11	0.029	26.4	I
141	860	16.7	46.98	0.02	0.006	28.08	I
146	892	14.71	20.48	0.04	0.015	37.5	I
141	863	3.65	20.79	0.01	0.004	39.83	I
112	681	13.99	21.82	0.04	0.023	57.5	I
169S	1033	3.75	89.1	0.02	0.013	64.36	I
169S	1034	3.79	115	0.01	0.015	150.5	I

‘Type II’ sediments are composed of high percentages (>65 wt%) of carbonate and generally have much lower ratios of OC to carbonate than Type I sites (Table 2) as well as minimal (<10%) reduction in sulfate. Because of the limited extent of net sulfate reduction, low pore fluid alkalinity, and pore fluid [Ca] that increase with depth, we infer that essentially all AC at Type II sites is generated from recrystallization of primary sedimentary carbonate, rather than net precipitation via remineralization of organic matter. Without a mechanism to offset the δ13C of the pore fluid ($\delta 13C_{PF\text{-}DIC}$), the recrystallized carbonate is indistinguishable from primary carbonate in terms of its δ13C signature.

Rates of AC formation in deep-sea sediments have been estimated using Sr concentration and $^{87}Sr/^{86}Sr$ values (Fantle and DePaolo, 2006; Richter and DePaolo, 1987, Richter and DePaolo, 1988). Others have used Ca and Sr concentrations, and $^{44}Ca/^{40}Ca$ ratios (Fantle and DePaolo, 2007, Sun and Turchyn, 2014, Turchyn and DePaolo, 2011). For Type II sites we use porewater Sr concentration data (Fig. 3) to estimate the formation rate of secondary (authigenic) carbonate. As shown by Fantle and DePaolo, 2006, Fantle and DePaolo, 2007, Sr concentrations give a reasonably good estimate of average recrystallization rates in the uppermost 80 m of most carbonate rich sections, although these estimates can be refined somewhat with use of Sr isotopes and Ca isotopes. For our purposes, we use only Sr concentration data because these data are available for a much larger number of sites. Our modeling approach for Type II sites involves an analytical solution to an advection–diffusion–reaction equation, yielding a single average value for the AC formation rate over a reaction length that is generally between 45 and 226 m.

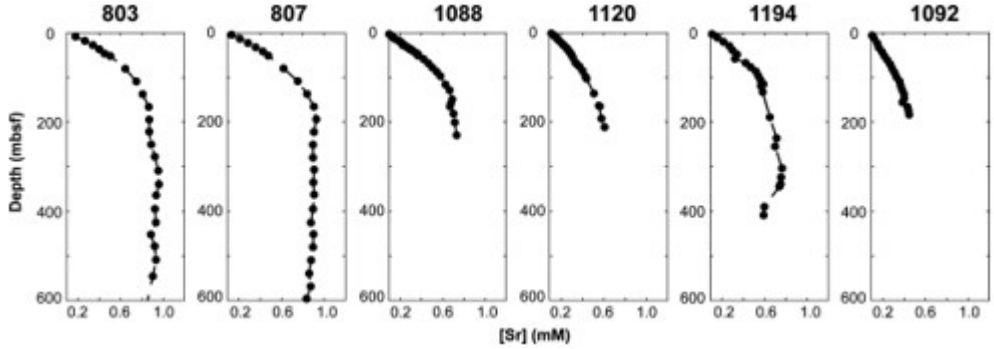

Fig. 3. Pore fluid strontium concentrations (mM) for examples of Type II sites.

For Type I sites, Sr concentration and isotopic data are much more complicated to interpret (e.g. Turchyn and DePaolo, 2011) because of Sr sourcing to pore waters via alteration of volcanic ash and detrital non-carbonate minerals (Hawkesworth and Elderfield, 1978). For Type I sites with available Sr pore fluid data, only two sites (618 and 892) have Sr pore fluid profiles which plateau at depth and therefore allow for the calculation of a reaction length. Because we expect net additions of AC from Type I sites due to the higher pore fluid alkalinity, an appropriate means of estimating this

component is by using pore fluid Ca concentrations. Although Ca is involved in other reactions, changes in calcium should be mainly due to the formation and dissolution of carbonates. Consequently, we use a similar advection–diffusion–reaction model utilizing porewater calcium concentrations, wherein we calculate advection and diffusion terms numerically from calcium concentrations, then invert for AC formation rate as a function of depth. We calculate fluxes from rates via integration to 80 m below the seafloor (mbsf). This captures the depth range of AC production that is likely to affect the global value of $\delta 13C_{M\text{-}DIC}$, taking into account that the characteristic diffusion time of DIC in porefluids over an 80 m depth interval is roughly equal to the seawater residence time of M-DIC (ca. 10^5 yr). More details and discussion of the models used are provided in the Supplemental Material.

2.2.2. Relative carbon burial fluxes

We compare the total rate of AC formation per unit area of seafloor to the overall burial rates of carbonate and OC at each site. The rate of AC formation per unit area of seafloor is obtained by integrating the rate per unit volume of sediment over depth from the seafloor to a prescribed depth in the sediment column. For Type II sites, BC is partially converted to AC, but there is (virtually) no carbonate added to the section during this process. For Type I sites, all of the AC formation calculated using our porefluid Ca concentration approach is added to the section during burial.

The total carbonate burial flux for each site is given by:

$$\text{Total Carbonate Flux}(\text{mol}\,\text{m}^{-2}\,\text{yr}^{-1}) = X_{carb}\,\rho_{sed}\,S\,(1-\phi)\,FW_{carb} \quad (6)$$

where S is sedimentation rate (m/yr), ϕ is average porosity, Xcarb is mass fraction of carbonate, ρsed is assumed to be 2700 kg/m^3 and FWcarb is the molar mass of $CaCO_3$(s). The burial flux of organic carbon is calculated similarly:

$$\text{Organic Carbon Flux}(\text{mol}\,\text{m}^{-2}\,\text{yr}^{-1}) = X_{org}\,\rho_{sed}\,S\,(1-\phi)\,FW_{C} \quad (7)$$

where Xorg is the volume fraction of organic carbon and FWC is the molar mass of elemental carbon. We calculate ϕ, Xcarb and Xorg over an 80 m averaging interval. Although these parameters can change considerably over this length scale, it is the depth-integrated flux, not the depth-specific rate that we need to estimate. The authigenic carbonate flux is the difference between the total carbonate flux and the biogenic carbonate flux. The sum of the three individual fluxes is equal to the total C burial flux (mol m^{-2} yr^{-1}) (Tables SI.2.1-1 and SI.2.2-1). The fractions in Fig. 6 are computed as follows:

$$f_{OC} = \text{organic carbon flux} / \text{total C flux} \quad (8)$$

$$f_{BC} = \text{biogenic carbonate flux} / \text{total C flux} \quad (9)$$

$$f_{AC} = \text{authigenic carbonate flux} / \text{total C flux} \quad (10)$$

2.3. Carbon isotope measurements

Carbon isotope compositions of bulk carbonates for sites 807 and 1082 were measured at the Center for Stable Isotope Biogeochemistry Laboratory at the University of California, Berkeley. Measurements were made on a GV IsoPrime mass spectrometer with Dual Inlet MultiCarb system using 10–100 µg powdered samples, reported using the Vienna Pee Dee Belemnite standard (V-PDB). Long-term precision is ±0.05‰ (1 s.d.).

3. Results & discussion

3.1. Sedimentary fractions of authigenic carbonate (fAC)

For reference, a typical sedimentation rate at many high-carbonate sites is roughly 20 m Myr^{-1}, which corresponds to 350 mmol C m^{-2} yr^{-1} assuming porosity is 0.7 and X_{carb} = 0.9. In contrast, net rates of AC formation for Type I sites generally range from 0 to 55.4 mmol m^{-3} yr^{-1} (Fig. 4), corresponding to median and maximum fluxes of 0.3 and 25.4 mmol m^{-2} yr^{-1}, respectively (Table S-1), or 10–10^3 times smaller than a typical carbonate depositional flux. The larger Type I AC fluxes are found in sites located closer to shelf and slope areas and correspond to higher rates of sedimentation and sulfate reduction (Canfield, 1991). A key characteristic of the Type I sites is that even for those sites with higher AC fluxes (Table S-1) the f_{AC} values are very small (Fig. 5). For example, site 1082 has one of the highest AC fluxes of 2.4 mmol m^{-2} yr^{-1}, but an f_{AC} value of only 0.004 because of the high sedimentation rate, including sedimentation of both OC and BC. Similarly, site 618, with a maximum flux roughly two orders of magnitude higher than the median, has the highest f_{AC}value, which is still only 0.014. These AC fluxes and f_{AC} values are on average much smaller than the fluxes calculated for carbonate-rich sections.

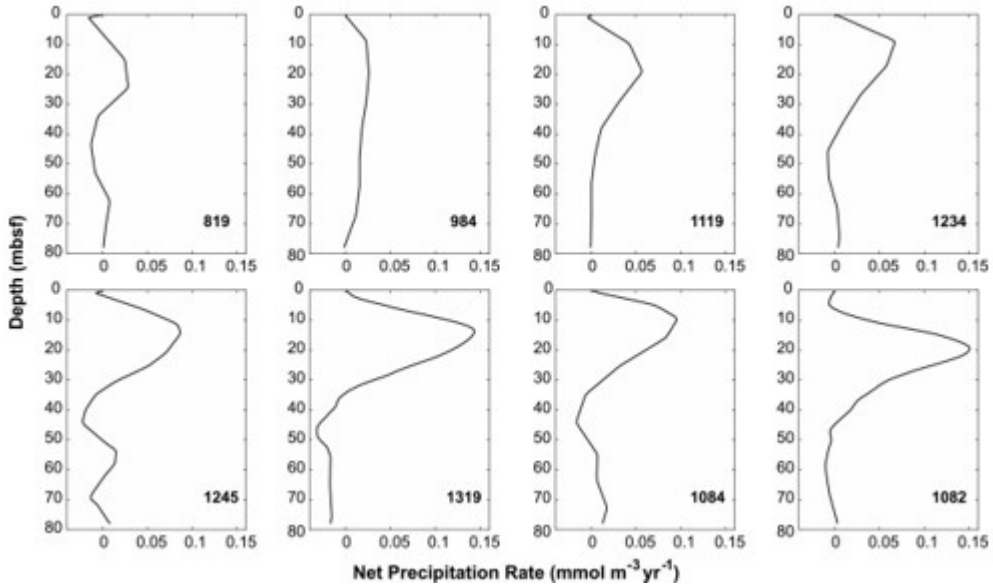

Fig. 4. Type I sites with high net precipitation rates of authigenic carbonate and typical depths of maximum rates (~10–20 mbsf).

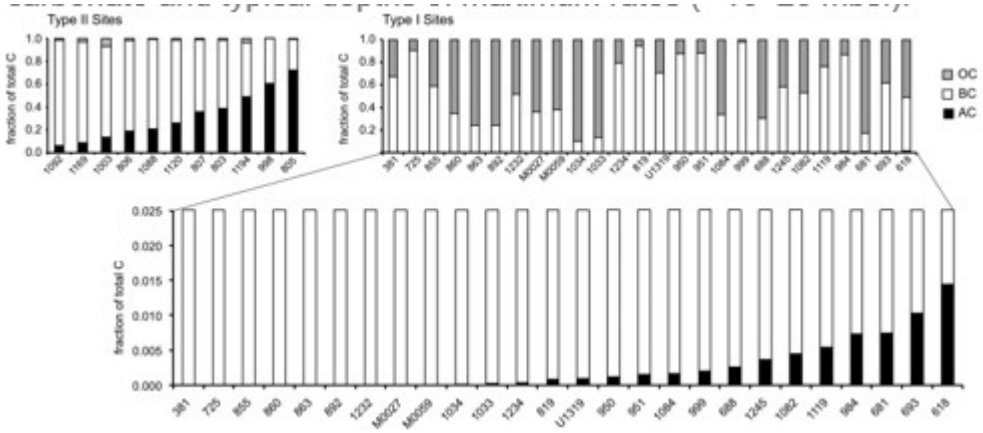

Fig. 5. Stacked bars showing sedimentary carbon fractions (AC = authigenic carbonate (black), BC = biogenic carbonate (white), OC = organic carbon (grey)) for each site, separated by site type. Note the lower panel is inset of Type I plot showing fractions 0 to 0.025 which cannot be seen on coarser scale diagram.

For Type II sites, the calculated reaction length (L), sedimentation rate (S), percent calcite, percent organic carbon, and model AC formation rates (= "recrystallization rates," R) are listed in Table S-2. The recrystallization rates are all smaller than 0.2 Myr^{-1}. The fitting of Sr concentration for all sites is shown in Supplementary Fig. S-1. A key characteristic of Type II sites is that the rate of AC formation can be quite high (up to 126 $mmol\,m^{-2}\,yr^{-1}$), which is a substantial fraction of the typical total carbonate burial rate, and corresponds to f_{AC} values of up to 0.72.

The relative authigenic, organic and biogenic carbon burial fractions for the sites analyzed are summarized in Fig. 6. Depth-dependent rates for Type I sites with highest AC precipitation rates are shown in Fig. 4 for all but site 618, which is discussed in Section 3.2.3.1. These sites all share similar depths of maximum AC production, roughly 10–20 m below the seafloor. For Type I sites, the relative burial fractions of biogenic carbonate and organic carbon vary over a large range (Fig. 6) but the corresponding burial fraction of AC is small (Fig. 5); in all cases less than about 0.02 and in most cases less than 0.01. Reimers et al. (1996), in their study of uppermost sediments in the Santa Barbara Basin, also found that in spite of significant increases in pH and carbonate alkalinity, the increase in authigenic calcite in sediments only increased the sedimentary carbonate content by 0.1%.

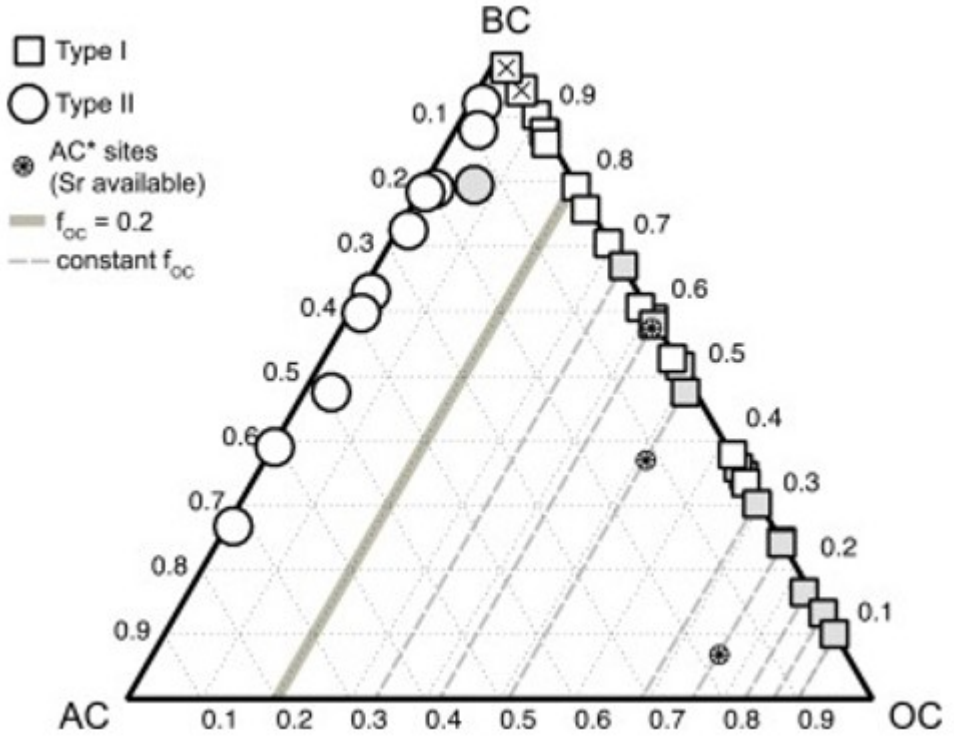

Fig. 6. Ternary plot showing relative sedimentary carbon fractions (f) of authigenic carbonate (AC), biogenic carbonate (BC), and organic (OC) carbon for Type I sites (squares) and Type II (circles). Grey shading indicates sites representing localized environments discussed in section 3.2.3. Squares with 'X' indicate sites 819 and 999, which have <65 wt% carbonate and OC/(AC + BC) ratios <0.1 and therefore do not fit squarely into Type I/II classification. Small circles with '*' show sedimentary carbon fractions for sites 618, 892, 1245, where estimates of AC* due to recrystallization can be calculated (Sr data available and Sr changes with depth indicative of recrystallization). Solid grey line denotes constant f_{OC} of 0.2 (estimate of modern value). Dashed grey lines denote constant f_{OC} values corresponding to sites discussed in section 3.2.3, indicating the theoretical range of f_{AC} and f_{BC} values as a function of extent of recrystallization.

For Type II sites, because of the small extent of organic carbon oxidation inferred from pore fluid profiles, we expect the PF-DIC and therefore AC to have virtually the same δ13C as BC (i.e., fAC∗=0) unless there are other means of resetting the $\delta 13C_{PF\text{-}DIC}$, which we explore in section 3.2. Overall, our initial analysis leads to the conclusion that AC formation in late Cenozoic marine sediments has a negligible impact on the global δ13C balance, regardless of depositional environment.

3.2. Evidence from δ13C

3.2.1. Type I approach

As a check on our results, we compare $\delta 13C_{PF\text{-}DIC}$ and carbonate δ13C values at sites where data are available to evaluate AC*/BC. At site 1082, complete sulfate reduction coincides with the depth of minimum $\delta 13C_{PF\text{-}DIC}$ (Fig. 7) demonstrating that the porefluid δ13C approaches that of oxidized organic matter. Porefluid calcium approaches a plateau at ~20 mbsf, indicating no net precipitation below this depth.

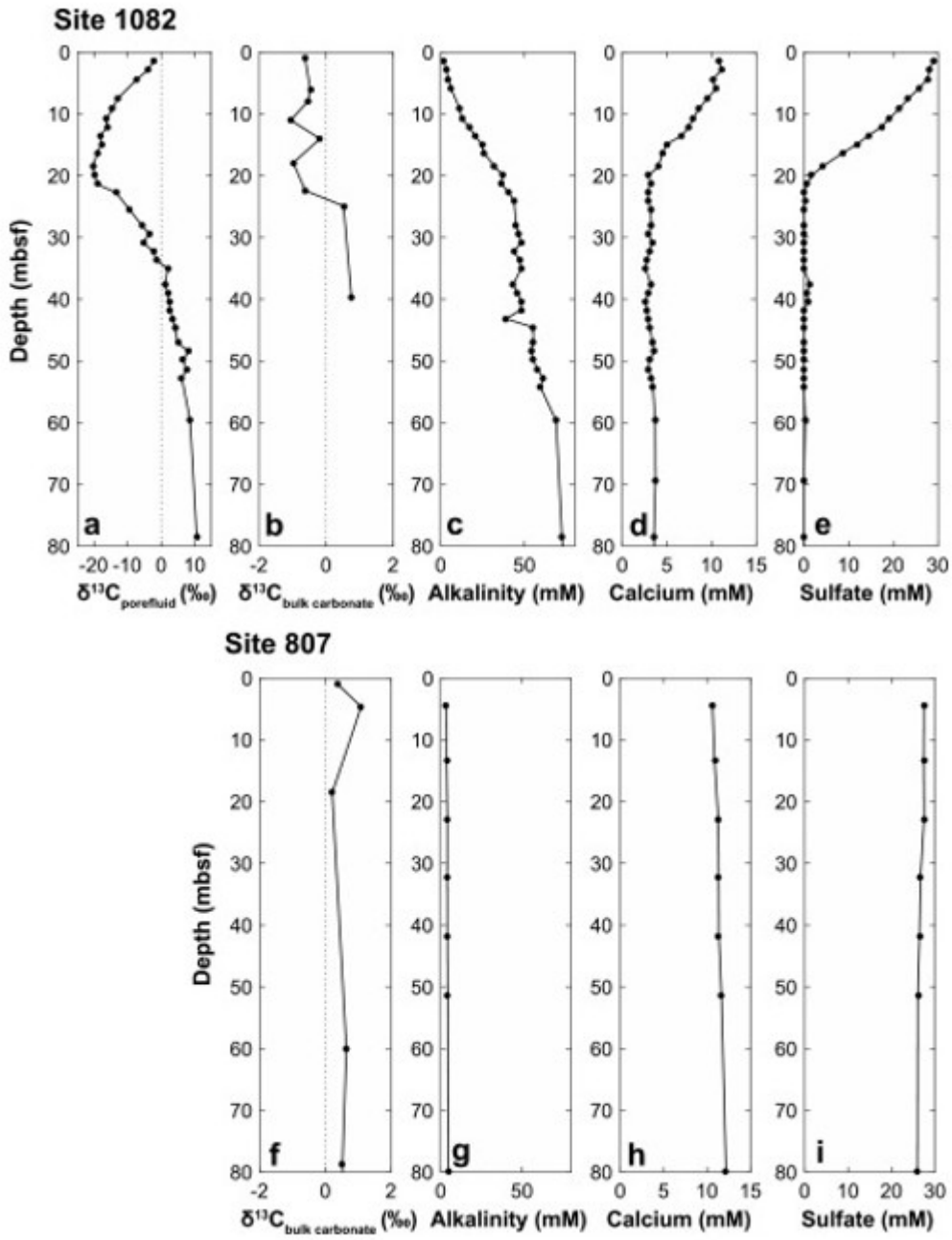

Fig. 7. Pore fluid bulk carbonate chemistry of Type I and Type II sites 1082 and 807, respectively. (a) Site 1082 pore fluid carbon isotopes from Moore et al. (2004); (b) Isotopic composition of bulk carbonates from site 1082 (this study); (c), (d) and (e) Site 1082 pore fluid data from Wefer et al. (1998); (f) Isotopic composition of bulk carbonates from Site 807 (this study); (g), (h) and (i) Site 807 pore fluid data from Kroenke et al. (1991).

If we assume that all AC at site 1082 precipitates with the $\delta 13C_{PF\text{-}DIC}$ composition of −20, the small average isotopic shift from M-DIC values in the bulk carbonate, which averages −0.35 (Fig. 7), requires that fAC be small, close to the value of 0.004 over the top 80 m calculated from our approach. The low δ13C of PF-DIC (Fig. 7) also confirms the inferences of Teichert et al. (2009), based on similar sections from Leg 204,

and Turchyn and DePaolo (2011), based on Sites 984 and 1082, that dissolution rates are exceptionally low in the parts of sections undergoing maximum sulfate reduction and secondary carbonate precipitation. In spite of isotopically depleted pore fluids of site 1082, we do not see a significant shift in the carbonate δ13C because of such low AC/BC.

3.2.2. Type II approach

Site 807, a Type II site, exhibits a <2 mM decrease in porewater sulfate relative to modern seawater values (28 mM) over an interval of 100 m (Kroenke et al., 1991). Although sulfate is not the only terminal electron acceptor that can be utilized in the remineralization of organic matter, we would expect an increase in pore fluid alkalinity to reflect other anaerobic oxidation pathways as well, which is not observed (Fig. 7). Although pore fluid δ13C are not available for site 807, the bulk carbonate isotopic composition that we measure (Fig. 7) can also provide insight into the carbon isotopic composition of the pore fluid. Our modeling suggests that the AC fraction at site 807 is ~0.36. If f_{AC}* were significant, the bulk carbonate isotopes should be noticeably offset from $\delta 13C_{M\text{-}DIC}$, which is not the case (Fig. 7). If we assume the biogenic carbonate is ±0.3‰, then the value of ΔAC is at most ±2.2‰. Other sites with minimal alkalinity production in the pore fluids and elevated sulfate concentrations throughout likely also have negligible f_{AC}.

3.2.3. Localized environments

In the following discussion we evaluate whether a high AC*/BC ratio is possible in modern marine sediments, and if so, what specific conditions allow for it. Although not globally representative, we look at sites in more extreme localized environments than those of sites 1082 and 807 that may be representative of different paleoenvironments. We focus on carbonate-dominant site 1003 (Bahamas Transect) as well as lower-carbonate sites with high pore fluid alkalinity thought to be producing AC today. These sites include those in close proximity to gas hydrates and/or methane seeps (Sites 681 and 688, Peru Continental Margin; Sites 892 and 1245, Cascadia Margin) and sites located in anoxic bottom waters(Sites 1033 and 1034, Saanich Inlet; Site 618, Orca Basin in Gulf of Mexico; Site 381, Black Sea).

3.2.3.1. Anoxic bottom water

Site 618 is located beneath 200 m of hypersaline brine in anoxic bottom waters of the Orca Basin (Bouma et al., 1986). Because of high and variable porewater salinity, our methodology is not necessarily appropriate for estimating AC formation rates. By correcting Ca to Cl concentrations (where M^{corr} = M(z)/(Cl(z)/Cl(o))), it is evident there is not a significant net change in Ca independent of the salinity gradient. However, Sr^{corr} reaches a plateau at ~50 m (Fig. S-3). If this trend reflects recrystallization, then f_{AC} would be 0.12, with fBC = 0.37 (Fig. 6). In this section, hydrates and gas pockets with up to 98% methane (Bouma et al., 1986) provide low-δ13C carbon, with

CH_4 gas samples averaging −73.5‰. Anaerobic oxidation of methane (AOM) in these sediments could very well promote high AC*/BC. It is noteworthy that this site also has fOC = 0.51, and therefore production of low-δ13C carbonate is still associated with burial conditions that would be expected to produce increasing atmospheric O_2 if applied globally.

Sites 1033 and 1034 are found in anoxic bottom waters of the Saanich Inlet, with alkalinity reaching ~80 and 100 mM, respectively, by 50 mbsf (Fig. S-8). Our calculations reveal that there is no net AC formation in these sections when averaged over the top 80 m, due to dissolution over the 50–80 m interval. These sites are another example of where the AC*/BC ratio may be significant. As with Site 681, these sites also have fOC≈ 0.90 (Fig. 6) and hence the low-δ13C AC would be associated with high rates of OC burial.

3.2.3.2. Carbonate platforms and periplatform sediments

Carbonate platforms are of particular interest because they may represent the modern sedimentary environment that most closely matches those in the geologic record prior to the Jurassic (Saltzman and Thomas, 2012). Site 1003 of the Bahamas resembles other Type II sites in its low ratio of OC to total carbonate (Table 2), relatively low deposition rate, and is roughly 94% carbonate by mass (however, >50% is aragonite). As highlighted by Swart and Eberli (2005) and Eberli et al. (1997), platform and periplatform carbonate sediments differ from pelagic sediments in key ways. One is that the dominant mineralogy of the primary carbonate is aragonite rather than calcite, and the other is that seawater flows through the system horizontally so that it is not possible to fully capture the pore-fluid interaction with the solid using a one-dimensional model. Bulk carbonates measure +1 to +5‰ (Swart and Eberli, 2005), but interpreting the δ13C of solids at this site is complicated, as it is not clear the extent to which this signal is from banktop-sourced material or *in situ* alteration. Downcore changes in mineralogy suggest a substantial amount of recrystallization. This section may represent one model for high AC*/BC, but also constitutes an environment where fOC is much lower than 0.2 (Fig. 6).

3.2.3.3. Continental margin sites

Many continental margin sites, including the Peru and Cascadian margins, have been studied for their authigenic carbonate production. These sites occupy regions of gas hydrate formation-dissociation and produce AC that can have both low and high δ13C. Meister et al. (2007) report “soft sediment” solid δ13C values from the Peru Margin ranging from −17.01 to +4.83 in core 681 (reoccupied during Leg 201 as core 1229), with dolomite samples from this core ranging from −13.6 to +6.09. Site 688, also on the Peru margin, shows porefluid Ca and Mg behavior indicative of net precipitation of low-Mg calcite or aragonite followed by dolomitization at depth. As of 1988, Site 688 had the highest alkalinity ever recorded in the Ocean Drilling Program (Suess et al., 1988). Increasingly lower chlorinity with depth as evidence of gas hydrate dissociation suggests this alkalinity

increase is the result of CH_4oxidation. Although carbonate δ13C data are not available to the best of the authors' knowledge, the incorporation of methane-derived δ13C into the dolomicrite found at this site would likely promote high fAC*.

Site 1245 on the Cascadian margin shows a range of δ13C in the PF-DIC, of ~−20 to ~+1 within the top 100 m (Tréhu et al., 2003), with the isotopic minimum coeval with sulfate depletion (Fig. S-9), similar to site 1082. Pore fluid alkalinity also reaches ~70 mM by 100 m, concurrent with a spike in dissolved HPO4−, suggesting that organic matter remineralization rather than AOM is the main contributor to the depleted fluid composition. Strontium concentrations change very little with depth, indicating that recrystallization is not an important process in forming authigenic calcite at this site. Net formation of authigenic calcite comprises less than 1% of the total sedimentary carbonate at the site according to our calculations. Near-complete sulfate removal (from 24.7 mM to 0.4 mM) occurs with a concurrent drawdown in Ca from 10.3 mM to 3.7 mM over the top ~12 m, after which both sulfate and calcium remain constant with depth (Fig. S-9). Tréhu et al. (2003) note AC forming in clay-rich layers as discrete Mg-calcite nodules (likely high-Mg calcite) in the upper ~45 m of sediment. Neither mineralogical analyses nor pore fluid chemistry suggest dolomite precipitation as a dominant authigenic phase at site 1245. Similar pore fluid chemistry and fractions of total carbonate to that of site 1082 (Table S-1 and Fig. 7) suggests the overall effect of organic carbon remineralization on the δ13C of total carbonate is small.

ODP site 892, located on Hydrate Ridge of the Cascadian Margin, has both aragonite layers and high Mg-calcite cement inter-grown with gas hydrates (Bohrmann et al., 1998). In contrast to site 1245, the Ca concentrations at site 892 increase with depth as Mg concentrations decrease (Fig. S-6). Along with increasing Sr concentrations with depth, these geochemical trends suggest the replacement of aragonite (into which Sr preferentially partitions) with high-Mg calcite. This interpretation is consistent with carbon and oxygen isotope data from Bohrmann et al. (1998), linking formation of the high Mg-calcite with the dissociation of the methane hydrates. There may be no net addition of AC at this site, but if we apply our Sr method to estimate recrystallization, our calculations yield f_{AC} of 0.165 (Fig. 6), over two times the amount of biogenic or primary carbonate present. With δ13C of carbonates in the range −40.6 to −54.2 (Bohrmann et al., 1998), this site is an example of high AC*/BC.

3.3. Conditions of AC* production

We have explored sediment cores that represent many different depositional environments, some of which are thought to have been more prevalent in the past. We acknowledge that our findings are limited by the extent to which sedimentary processes today may have been active in various paleoenvironments, and that the geologic record is incomplete. Despite this

uncertainty, there are specific observations that help elucidate the role of AC in the global carbon isotope balance through geologic time. The sites discussed in the preceding sections allow us to identify where and how authigenic carbonate could make up an isotopically significant fraction of total sedimentary carbon.

Today, it appears as though large fAC_* can be generated via AOM at or near sites of gas hydrate dissociation, as shown in sites 681 and 688 of the Peru Margin, site 892 of the Cascadian Margin, and site 618 of the anoxic Orca Basin. Sites 1082 or 1245, in which there is evidence of organic matter remineralization but not AOM, have a very small shift in the bulk carbonate solid δ13C composition in spite of isotopically depleted pore fluids. High rates of organic matter remineralization and AC production at sites such as these are countered in their isotopic effect by high biogenic carbonate (or primary sedimentary carbonate) fractions with δ13C very close to that of M-DIC.

Carbonate platforms and periplatform sediments may be a key, and somewhat complicated, aspect of the authigenic carbonate story. It is not clear in our analysis that a significant amount AC* is produced *in situ* at site 1003, in spite of carbonate platforms showing extensive diagenesis (Eberli et al., 1997). The mixing of banktop sediment with pelagic calcifiers causes an overall diluting of isotopically offset signals. If the source of the high porefluid alkalinity in periplatform sediments is a mixture of recrystallizing banktop and biogenic sediment as well as from the remineralization of organic matter, arguably the high δ13C signature in the bulk carbonate will be slowly shifted towards low δ13C values. Given how difficult it is to offset the bulk carbonate δ13C in a site like 1082, which has much lower overall carbonate than site 1003, it seems unlikely that these periplatform sediments can remineralize enough organic matter to create high AC*/BC. However, fractionation of DIC during aragonite precipitation and distillation effects during photosynthesis (Swart and Eberli, 2005) suggest that the banktop itself could be an important locus of AC precipitation.

3.4. AC* formation in Earth history

During past times of ocean anoxia, seafloor carbonate precipitates are thought to be widespread (Grotzinger and Knoll, 1995, Higgins et al., 2009, Pruss et al., 2006). If past seafloor carbonates formed in similar environments to the gas hydrate continental marginsseen today, they may have affected $\delta13C_{M\text{-}DIC}$ even if they weren't widespread. If oceans were anoxic, then supersaturated bottom waters could have promoted the expansion of these carbonates beyond the amount proportional to initial alkalinity generated via CH_4-oxidation. It is possible that following production of carbonate from CH_4-oxidation, δ13C of the precipitates would shortly evolve back to $\delta13C_{M\text{-}DIC}$. Therefore, it is unclear whether extensive seafloor precipitation of carbonates could perturb $\delta13C_{M\text{-}DIC}$, even during anoxic

intervals. It is expected that on short timescales (10^4–10^5 yr), biogenic carbonate production would diminish when waters were anoxic (Pruss et al., 2006), shifting the AC/BC ratio higher.

Total size of the DIC pool is expected to be an important factor in determining the effect of AC precipitation on $\delta13C_{M\text{-}DIC}$. The M-DIC reservoir has become smaller since the Proterozoic, and so has the magnitude of variations in $\delta13C_{M\text{-}DIC}$ (Bartley and Kah, 2004). Bartley and Kah (2004) argue that coupling of organic matter and biogenic carbonate production with the proliferation of calcifying nannoplankton created isotopic buffering against changes to $\delta13C_{M\text{-}DIC}$. This link suggests perturbations to $\delta13C_{M\text{-}DIC}$ due to AC were more likely in the Precambrian and intervals in the Phanerozoic (e.g., early Cambrian) when calcifying organisms were not as prolific as they are in modern oceans.

3.5. Global versus local δ13C

The use of δ13C to interpret global paleoenvironment hinges on the assumption that what is recorded represents a global $\delta13C_{M\text{-}DIC}$ value. The pre-Jurassic record is generally sourced from shallow-water sediments, which in the modern ocean show atypical high AC*/BC. Hence, it is possible that pre-Jurassic δ13C might be reflecting an integrated signal of local conditions in the water column and/or AC production with $\delta13C_{PF\text{-}DIC}$, and therefore would not necessarily appear geochemically or petrologically distinct from carbonates reflecting global marine conditions aside from their δ13C composition.

4. Conclusions

In this study, we sought to use the abundant and systematic pore fluid chemical data available from the deep sea drilling archive to evaluate the potential role of authigenic carbonate formation in marine sediments in affecting the carbon isotopic composition of marine DIC. Our specific approach is to evaluate the *relative* rates of formation/burial of biogenic (or primary sedimentary), organic, and authigenic carbon (BC:OC:AC) in an array of late Cenozoic marine sedimentary environments chosen to encompass a range of sediment compositions, sedimentation rates, oxygenation conditions, and water depths. The goal was to estimate the likely range of modern proportions of different carbon burial rates, and to determine what site characteristics, if any, would be most favorable to making AC a major factor in the δ13C budget. Such site characteristics might be rare in the modern oceans but could have been more prevalent in Mesozoic, Paleozoic, or Precambrianoceans.

In analyzing modern sites and considering possible differences between modern sedimentary environments and those of the past, we find only a few characteristics that can change in a way that would promote the needed formation of AC* (AC that is isotopically distinct from BC). One possibility is to have an OC/BC ratio substantially higher than the long-term average of

0.2 with an AC/BC ratio of at least 0.1. This, however, does not change the idea that high $\delta 13C_{M\text{-}DIC}$ values correspond to excess organic carbon burial, which is already accounted for in the isotope model with only BC and OC.

An environment that might be expected to have significant AC* production, but does not, is site 1082, a continental margin site in the South Atlantic. This site might be expected to have a high AC*/BC burial ratio because of its location in an upwelling zone, high pore fluid alkalinity, complete sulfate removal, and high X_{oc}/X_{carb} ratio. However, our analysis shows that AC*/BC is two orders of magnitude too small to be significant at this site. The high carbonate site 807 (Ontong-Java Plateau), in contrast, is an example of where there is high AC/BC, but no means of creating AC*. These two site types have been widespread since the Jurassic, and so for this span of time, authigenic carbonate likely has had no material effect on the δ13C of the ocean. Prior to this, understanding the role of AC is more difficult because the record is derived mainly from shallow marine environments, for which diagenetic processes are typically different in comparison to deep sea environments, and which can record δ13C values that deviate from the global ocean (Saltzman and Thomas, 2012). Our difficulty in finding example environments that would be favorable for making AC* a significant component of the global δ13C balance leads us to conclude that such environments may not exist.

We explored sites in the ODP database that, although highly localized today, perhaps hosted extreme enough conditions to have high AC*/BC. The most convincing locus of high AC*/BC is in continental margins where dolomitization and other carbonate recrystallization occurs with gas hydrate formation-dissociation and where anaerobic methane oxidation is dominant. Restricted or semi-restricted basins with anoxic bottom waters could also be sites of high AC*/BC, but it is likely that methane, rather than organic matter, needs to be the main source of isotopically light δ13C for AC* production. Finally, carbonate platforms and periplatform sediments may be settings of high AC*/BC production, but the interpretation of bulk carbonate δ13C requires a different model that accounts for additional factors.

On long timescales (order 10 My), if more extreme environments like those explored above were globally extensive, it is possible that AC production could influence the δ13C budget. However, if pelagic calcifying organisms comprise significant fractions of total sedimentary carbon, as is thought to be the case for much of the Phanerozoic, it is unlikely that these high AC*/BC conditions were sufficiently widespread. Prior to the proliferation of calcifying organisms, and specifically in the Precambrian, these environments could have been more likely given the decreased isotopic buffering effect provided by biogenic carbonate.

It is not clear that a steady state approximation is appropriate for interpreting isotope excursions. It is possible that if isotope excursions are

reflecting authigenic carbonate, they are a local signal, such as those observed today in carbonate platforms and AOM-dominant environments with low BC. Extensive AC formation on timescales of observed excursions is possible only with equally transient phenomena such as global methane hydrate release, as is thought to have occurred at the Paleocene–Eocene boundary (Dickens et al., 1995). This possibility, however, implies that any isotopic effect of authigenic carbonate production is secondary to the impact of an environmental perturbation on the δ13C of the ocean and therefore may not require inclusion in an isotopic mass balance model.

Acknowledgments

The authors thank David Fike, Galen Halverson, and John Higgins, whose insightful comments helped improve the manuscript considerably. The authors also thank Wenbo Yang for measuring carbon isotopes of bulk carbonate samples and Holly Barnhart for helping to compile carbon isotope data for Fig. 1. This research was supported by the U.S. Department of Energy, Office of Science, Office of Basic Energy Sciences, Chemical Sciences, Geosciences, and Biosciences Division, under Award Number DE-AC02-05CH11231.

References

Arthur et al., 1988

M.A. Arthur, W.E. Dean, L.M. Pratt**Geochemical and climatic effects of increased marine organic carbon burial at the Cenomanian/Turonian boundary**

Nature, 335 (6192) (1988), pp. 714-717

Bartley and Kah, 2004

J.K. Bartley, L.C. Kah**Marine carbon reservoir, C_{org}–C_{carb} coupling, and the evolution of the Proterozoic carbon cycle**

Geology, 32 (2) (2004), pp. 129-132

Berner and Canfield, 1989

R.A. Berner, D.E. Canfield**A new model for atmospheric oxygen over Phanerozoic time**

Am. J. Sci., 289 (4) (1989), pp. 333-361

Berner and Maasch, 1996

R.A. Berner, K.A. Maasch**Chemical weathering and controls on atmospheric O_2 and CO_2: fundamental principles were enunciated by J.J. Ebelmen in 1845**

Geochim. Cosmochim. Acta, 60 (9) (1996), pp. 1633-1637

Berner and Petsch, 1998

R.A. Berner, S.T. Petsch**The sulfur cycle and atmospheric oxygen**

Science, 282 (5393) (1998), pp. 1426-1427

Bohrmann et al., 1998

G. Bohrmann, J. Greinert, E. Suess, M. Torres**Authigenic carbonates from the Cascadia subduction zone and their relation to gas hydrate stability**

Geology, 26 (7) (1998), pp. 647-650

Bouma et al., 1986

A.H. Bouma, J.M. Coleman, A.W. Meyer, *et al.***Deep Sea Drilling Program**

Initial Reports, vol. 96, U.S. Govt. Printing Office, Washington (1986)

Canfield, 1991

D.E. Canfield**Sulfate reduction in deep-sea sediments**

Am. J. Sci., 291 (2) (1991), pp. 177-188

Canfield and Kump, 2013

D.E. Canfield, L.R. Kump**Carbon cycle makeover**

Science, 339 (6119) (2013), pp. 533-534

Canfield and Teske, 1996

D.E. Canfield, A. Teske**Late Proterozoic rise in atmospheric oxygen concentration inferred from phylogenetic and sulphur-isotope studies**

Nature, 382 (6587) (1996), pp. 127-132

Derry, 2014

L.A. Derry**Organic carbon cycling and the lithosphere**

Treatise on Geochemistry (second edition), Elsevier Inc (2014)

Dickens et al., 1995

G.R. Dickens, J.R. O'Neil, D.K. Rea, R.M. Owen**Dissociation of oceanic methane hydrate as a cause of the carbon isotope excursion at the end of the Paleocene**

Paleoceanography, 10 (6) (1995), pp. 965-971

Eberli et al., 1997

G.P. Eberli, P.K. Swart, M.J. Malone, *et al.***Proceedings of the Ocean Drilling Program**

Initial Reports, vol. 166 (1997)

Fantle and DePaolo, 2006

M.S. Fantle, D.J. DePaolo**Sr isotopes and pore fluid chemistry in carbonate sediment of the Ontong Java Plateau: calcite**

recrystallization rates and evidence for a rapid rise in seawater Mg over the last 10 million years

Geochim. Cosmochim. Acta, 70 (15) (2006), pp. 3883-3904

Fantle and DePaolo, 2007

M.S. Fantle, D.J. DePaolo**Ca isotopes in carbonate sediment and pore fluid from ODP Site 807A: the Ca^{2+}(aq)–calcite equilibrium fractionation factor and calcite recrystallization rates in Pleistocene sediments**

Geochim. Cosmochim. Acta, 71 (10) (2007), pp. 2524-2546

Farquhar et al., 2001

J. Farquhar, J. Savarino, S. Airieau, M.H. Thiemens**Observation of wavelength-sensitive mass-independent sulfur isotope effects during SO_2photolysis: implications for the early atmosphere**

J. Geophys. Res., Planets, 106 (E12) (2001), pp. 32829-32839

Grotzinger and Knoll, 1995

J.P. Grotzinger, A.H. Knoll**Anomalous carbonate precipitates: is the Precambrian the key to the Permian?**

Palaios, 10 (6) (1995), pp. 578-596

Halverson et al., 2005

G.P. Halverson, P.F. Hoffman, D.P. Schrag, A.C. Maloof, A.H.N. Rice**Toward a Neoproterozoic composite carbon-isotope record**

Geol. Soc. Am. Bull., 117 (9–10) (2005), pp. 1181-1207

Hawkesworth and Elderfield, 1978

C.J. Hawkesworth, H. Elderfield**The strontium isotopic composition of interstitial waters from Sites 245 and 336 of the Deep Sea Drilling Project**

Earth Planet. Sci. Lett., 40 (3) (1978), pp. 423-432

Higgins et al., 2009

J.A. Higgins, W.W. Fischer, D.P. Schrag**Oxygenation of the ocean and sediments: consequences for the seafloor carbonate factory**

Earth Planet. Sci. Lett., 284 (1) (2009), pp. 25-33

Kroenke et al., 1991

L.W. Kroenke, W.H. Berger, T.R. Janecek**Proceedings of the Ocean Drilling Program**

Initial Reports, vol. 130 (1991)

Kump and Arthur, 1999

L.R. Kump, M.A. Arthur**Interpreting carbon-isotope excursions: carbonates and organic matter**

Chem. Geol., 161 (1) (1999), pp. 181-198

Lowenstein et al., 2014

T.K. Lowenstein, B. Kendall, A.D. Anbar**The geologic history of seawater**

Treatise on Geochemistry (second edition), Elsevier Inc (2014)

Marshall et al., 1997

J.D. Marshall, P.J. Brenchley, P. Mason, G.A. Wolff, R.A. Astini, L. Hints, T. Meid la**Global carbon isotopic events associated with mass extinction and glaciation in the late Ordovician**

Palaeogeogr. Palaeoclimatol. Palaeoecol., 132 (1–4) (1997), pp. 195-210

Meister et al., 2007

P. Meister, J.A. Mckenzie, C. Vasconcelos, S. Bernasconi, M. Frank, M. Gutjahr, D.P. Schrag**Dolomite formation in the dynamic deep biosphere: results from the Peru Margin**

Sedimentology, 54 (5) (2007), pp. 1007-1032

Moore et al., 2004

T.S. Moore, R.W. Murray, A.C. Kurtz, D.P. Schrag**Anaerobic methane oxidation and the formation of dolomite**

Earth Planet. Sci. Lett., 229 (1) (2004), pp. 141-154

Morse et al., 2007

J.W. Morse, R.S. Arvidson, A. Lüttge**Calcium carbonate formation and dissolution**

Chem. Rev., 107 (2) (2007), pp. 342-381

Payne et al., 2004

J.L. Payne, D.J. Lehrmann, J.Y. Wei, M.J. Orchard, D.P. Schrag, A.H. Knoll**Large perturbations of the carbon cycle during recovery from the end-Permian extinction**

Science, 305 (683) (2004), pp. 506-509

Pruss et al., 2006

S.B. Pruss, D.J. Bottjer, F.A. Corsetti, A. Baud**A global marine sedimentary response to the end-Permian mass extinction: examples from southern Turkey and the western United States**

Earth-Sci. Rev., 78 (3) (2006), pp. 193-206

Raven and Falkowski, 1999

J.A. Raven, P.G. Falkowski**Oceanic sinks for atmospheric CO_2**

Plant Cell Environ., 22 (6) (1999), pp. 741-755

Reimers et al., 1996

C.E. Reimers, K.C. Ruttenberg, D.E. Canfield, M.B. Christiansen, J.B. Martin**Porewater pH and authigenic phases formed in the uppermost sediments of the Santa Barbara Basin**

Geochim. Cosmochim. Acta, 60 (21) (1996), pp. 4037-4057

Retallack and Jahren, 2008

G.J. Retallack, A.H. Jahren**Methane release from igneous intrusion of coal during Late Permian extinction events**

J. Geol., 116 (1) (2008), pp. 1-20

Richter and DePaolo, 1987

F.M. Richter, D.J. DePaolo**Numerical models for diagenesis and the Neogene Sr isotopic evolution of seawater from DSDP Site 590B**

Earth Planet. Sci. Lett., 83 (1) (1987), pp. 27-38

Richter and DePaolo, 1988

F.M. Richter, D.J. DePaolo**Diagenesis and Sr isotopic evolution of seawater using data from DSDP 590B and 575**

Earth Planet. Sci. Lett., 90 (4) (1988), pp. 382-394

Saltzman, 2005

M.R. Saltzman**Phosphorus, nitrogen, and the redox evolution of the Paleozoic oceans**

Geology, 33 (7) (2005), pp. 573-576

Saltzman and Thomas, 2012

M.R. Saltzman, E. Thomas**Carbon isotope stratigraphy**

The Geologic Time Scale, vol. 1 (2012), pp. 207-232

Schidlowski et al., 1975

M. Schidlowski, R. Eichmann, C.E. Junge**Precambrian sedimentary carbonates: carbon and oxygen isotope geochemistry and implications for the terrestrial oxygen budget**

Precambrian Res., 2 (1) (1975), pp. 1-69

Schrag et al., 2013

D.P. Schrag, J.A. Higgins, F.A. Macdonald, D.T. Johnston**Authigenic carbonate and the history of the global carbon cycle**

Science, 339 (6119) (2013), pp. 540-543

Sephton et al., 2002

M.A. Sephton, C.V. Looy, R.J. Veefkind, H. Brinkhuis, J.W. De Leeuw, H. Visscher**Synchronous record of δ13C shifts in the oceans and atmosphere at the end of the Permian**

Spec. Pap., Geol. Soc. Am., 356 (2002), pp. 455-462

Shields and Veizer, 2002

G. Shields, J. Veizer**Precambrian marine carbonate isotope database: version 1.1**

Geochem. Geophys. Geosyst., 3 (6) (2002)

Suess et al., 1988

Suess, E., von Huene, R., et al., 1988. Proc. ODP, Init. Repts., 112: College Station, TX (Ocean Drilling Program). https://doi.org/10.2973/odp.proc.ir.112.1988.

Sun and Turchyn, 2014

X. Sun, A.V. Turchyn**Significant contribution of authigenic carbonate to marine carbon burial**

Nat. Geosci., 7 (3) (2014), p. 201

Swart and Eberli, 2005

P.K. Swart, G. Eberli**The nature of the δ13C of periplatform sediments: implications for stratigraphy and the global carbon cycle**

Sediment. Geol., 175 (2005), pp. 115-129

Teichert et al., 2009

B.M.A. Teichert, N. Gussone, M.E. Torres**Controls on calcium isotope fractionation in sedimentary porewaters**

Earth Planet. Sci. Lett., 279 (3) (2009), pp. 373-382

Tréhu et al., 2003

Tréhu, A.M., Bohrmann, G., Rack, F.R., Torres, M.E., et al., 2003. Proc. ODP, Init. Repts., 204: College Station, TX (Ocean Drilling Program). https://doi.org/10.2973/odp.proc.ir.204.2003.

Turchyn and DePaolo, 2011

A.V. Turchyn, D.J. DePaolo**Calcium isotope evidence for suppression of carbonate dissolution in carbonate-bearing organic-rich sediments**

Geochim. Cosmochim. Acta, 75 (22) (2011), pp. 7081-7098

Walter et al., 1993

L.M. Walter, S.A. Bischof, W.P. Patterson, T.W. Lyons, R.K. O'Nions, M. Gruszczynski, B.W.Sellwood, M.L. Coleman**Dissolution and recrystallization in**

modern shelf carbonates: evidence from pore water and solid phase chemistry

Philos. Trans. R. Soc., Math. Phys. Eng. Sci. (1993), pp. 27-36